Available online at www.sciencedirect.com
SCIENCE DIRECT
Bioorganic & Medicinal Chemistry Letters
Bioorganic & Medicinal Chemistry Letters 16 (2006) 1811–1815

Benzoxazole benzenesulfonamides are novel allosteric inhibitors of fructose-1,6-bisphosphatase with a distinct binding mode

Thomas W. von Geldern,[a,*] Chunqiu Lai,[a] Rebecca J. Gum,[a] Melissa Daly,[a] Chaohong Sun,[b] Elizabeth H. Fry[b] and Celerino Abad-Zapatero[b]

[a]*Metabolic Disease Research, GPRD, Abbott Laboratories, Abbott Park, IL 60064, USA*
[b]*Structural Biology Department, GPRD, Abbott Laboratories, Abbott Park, IL 60064, USA*

Received 22 November 2005; revised 4 January 2006; accepted 5 January 2006
Available online 25 January 2006

Abstract—We have identified benzoxazole benzenesulfonamide **1** as a novel allosteric inhibitor of fructose-1,6-bisphosphatase (FBPase-1). X-ray crystallographic and biological studies of **1** indicate a distinct binding mode that recapitulates features of several previously reported FBPase-1 inhibitor classes.

Glucose generation and glucose disposal are tightly regulated and balanced in order to maintain normal levels of circulating glucose. Disturbances in this balance can result in hyperglycemia or hypoglycemia. Fasting hyperglycemia is associated with increased gluconeogenesis[1] which is regulated by three key enzymes: phosphoenolpyruvate carboxykinase (PEPCK), glucose-6-phosphatase (G6Pase), and fructose-1,6-bisphosphatase (FBPase-1).[2] Changes in activity of any of these enzymes can cause abnormal hepatic glucose output. In diabetic patients and animal models of Type 2 diabetes (T2DM), the expression and activity of FBPase-1 is upregulated in liver, consequently increasing net glucose production.[3]

FBPase-1 is a homotetrameric protein existing in active (R) and inactive (T) conformational states. Regulation of enzymatic activity involves changes in conformation of the homotetramer between R and T states. Metal cations, fructose-1,6-bisphosphate (F-1,6-P), and fructose-6-phosphate (F-6-P) help to stabilize the R state. Adenosine-5-monophosphate (AMP) is a negative regulator of FBPase-1 activity, inducing a change from R to T state; while binding of fructose-2,6-bisphosphate (F-2,6-P) synergistically increases the binding and potency of AMP.[4]

Several previous reports have highlighted the potential of small molecule inhibitors of FBPase-1 for the treatment of T2DM (Fig. 1). Of particular note is the work

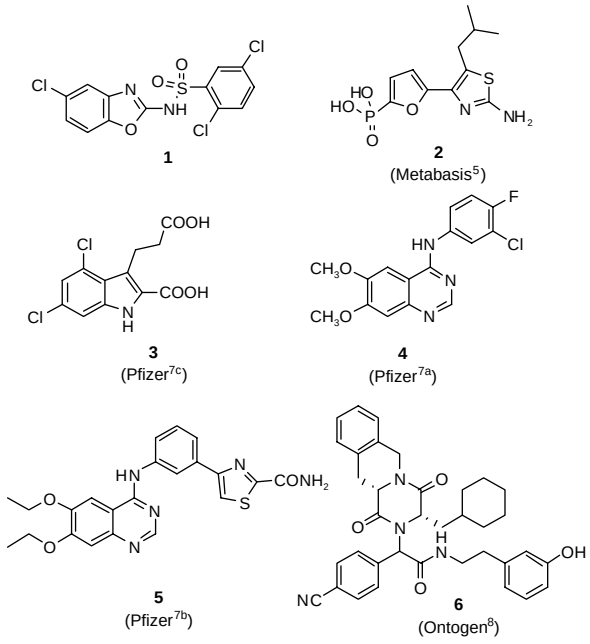

Figure 1. Small-molecule inhibitors of FBPase-1.

Keywords: Fructose-1,6-bisphosphatase; Enzyme inhibitor; Benzoxazole benzenesulfonamides; Allosteric regulation; X-ray crystallography.
* Corresponding author. Tel.: +1 847 937 9171; fax: +1 847 938 1674; e-mail: Thomas.vongeldern@abbott.com

0960-894X/$ - see front matter © 2006 Elsevier Ltd. All rights reserved.
doi:10.1016/j.bmcl.2006.01.015

of the Metabasis group to prepare a family of heteroaryl phosphonates as AMP-site allosteric inhibitors.[5] One such inhibitor, CS-917 (**2**), has demonstrated glucose-lowering activity in diabetic rodent models[5] and in patients,[6] providing important validation for this target. Pfizer[7] and Ontogen[8] have reported several other chemotypes, including indole dicarboxylic acids (**3**),[7a] anilinoquinazolines (**4**,**5**),[7b,c] and piperazinediones (**6**),[8] as FBPase inhibitors.

Our own high-throughput screen for FBPase-1 inhibitors identified a cluster of benzoxazole-2-benzenesulfonamides, of which compound **1** is representative. This high-throughput assay employed malachite green (MG) to detect free phosphate ion liberated when fructose-6-phosphate is produced from fructose-1,6-bisphosphate by the action of human FBPase-1.[9] In a confirmatory assay, production of fructose-6-phosphate is monitored in real time by coupling with phosphoglucose isomerase and glucose-6-phosphate dehydrogenase to give 6-phosphoglucono-δ-lactone.[10] The concomitant reduction of NADP to NADPH is monitored spectrofluorometrically. Sulfonamide **1** exhibits similar potency (IC_{50} = 3.4 μM using MG; = 4.0 μM in the 'coupled' format) in these two distinct assays of FBPase-1 activity (Fig. 2). The 'coupled' assay format produces time-resolved data that may be subjected to kinetic analysis; this analysis indicates a K_i of 1.1 ± 0.1 μM for compound **1**.

Compound **1** also functions as expected in a cellular model of glucose production (Fig. 3). In this assay, rat hepatoma cells are starved of nutrients, making them highly dependent on the processing of gluconeogenic precursors pyruvate and lactate to provide energy in the form of glucose. Glucose production is measured over a three-hour period; the decrease in glucose output

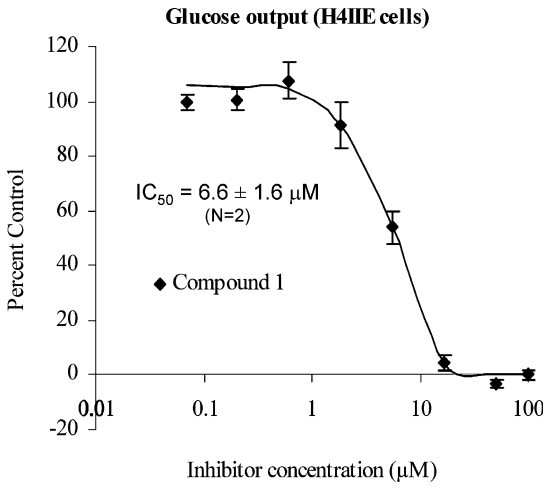

Figure 3. Effects of **1** on cellular glucose output.

that occurs with increasing doses of **1** is indicative of its ability to block gluconeogenesis by inhibiting FBPase-1. The potency in this functional assay (IC_{50} = 6.6 μM) is in line with its potency in the enzymatic assays.

FBPase-1 is a well-characterized enzyme, and the binding modes of a number of inhibitors are understood at the molecular level. Thus, it has been determined crystallographically that phosphonate **2**[5] and the indole diacid **3**[7c] both fill the AMP allosteric binding site. On the other hand, the second-generation anilinoquinazoline **5** displays a novel mode of inhibition,[7b] binding at the homotetramer subunit interface. X-ray studies indicate primary contacts between these anilinoquinazolines and the sidechains of Lys50 and His55; these interactions disrupt a loop that acts as part of the conformation switch regulating the transition between R and T states.

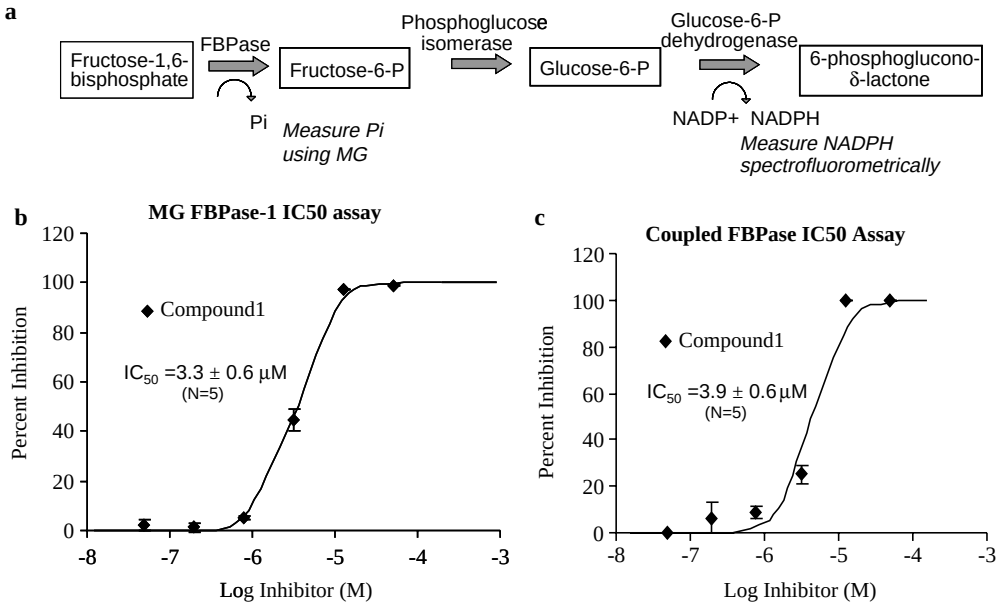

Figure 2. FBPase inhibitory activity of compound **1**. Panel a shows the enzymatic pathway and indicates the formats for the primary enzymatic assays of FBPase-1 inhibitory activity. Panel b shows IC_{50} data for the malachite green (MG) assay, measuring release of phosphate. Panel c shows data determined from continuous assay employing a coupled enzyme system to measure fructose-6-phosphate levels as NADP reduction. IC_{50} values in both assays are similar.

To gain a better understanding of the binding mode of our novel series, the crystal structure of **1** was determined with human FBPase.[11,12] Analysis of the structure (Fig. 4) reveals a novel binding mode for compound **1**. The stoichiometry of binding is one molecule of **1** per subunit (or 4 per FBPase tetramer); in this sense it is similar to compounds **2** and **3**, but distinct from **5** (which binds at a 2-per-tetramer ratio). The aryl ring of the benzenesulfonamide group fills a hydrophobic region defined by a series of residues including Val17, Leu30, Leu34, and Met177 on one side and Ala24, Gly26, and the methylenes of Glu20 on the other side. This hydrophobic zone sits just above a deep pocket that includes a set of polar sidechains and exposed backbone NHs. It is these polar groups that serve as a binding pocket to recognize the phosphate group of the allosteric inhibitor AMP. The aryl group blocks access to, but does not occupy, this phosphate binding pocket. This represents a novel solution to the problem of interacting with the AMP allosteric regulatory site; other AMP-competitive analogs, like **2** and **3**, contain functionality designed to interact directly with residues within the phosphate pocket (Fig. 4a). At the same time, the benzoxazole functionality of **1** pushes out into the subunit interface region. The hydrophobic nature of the aromatic ring on the benzoxazole is muted through a pi-stacking interaction with a second inhibitor molecule, occurring *trans*- across the subunit interface (Fig. 4b). While in the case of **1**, the benzoxazole substituent remains in this interface zone, making a contact with Met18, we have observed (data not shown) that larger substituents can sometimes make *trans*-contacts with a second FBPase subunit.

Any compound that simultaneously interacts with both the phosphate binding pocket and the subunit interface must find a way to 'duck under' a bridge (consisting of residues Ala24–Gly28) that blocks the gap between these two sites. Compound **1** solves this logistical problem by forming a dense network of hydrogen bonds between the sulfonamide moiety and the bridge (Fig. 4b). In particular, the oxygen atoms of the sulfonamide form H-bonds with the backbone amide NHs of Gly22, Gly29, and Leu30, while the sulfonamide NH interacts with the hydroxyl group of Thr31. This core interaction stabilizes the conformation of both protein and ligand, and positions the two substituents in the appropriate binding domains.

This crystallographically determined binding mode suggests several testable hypotheses regarding the inhibitory properties of **1**. Since **1** blocks access to the AMP allosteric binding site, it should be competitive with AMP as an inhibitor of FBPase-1. This is confirmed by the saturation transfer difference (std) NMR experiments[13] shown in Figure 5a. Using N^6-methyl AMP ($IC_{50} \sim 150\ \mu M$ in the coupled assay) as a probe molecule for the AMP site, saturation transfer from FBPase-1 to this ligand (top panel) is completely blocked (middle panel) by the AMP-mimetic ZMP ($IC_{50} = 15\ \mu M$ in the 'coupled' assay)[14] or by compound **1** (bottom panel), suggesting that both compete for the AMP binding site. Similarly, it is expected (and observed) that **1** does not compete with the alternative allosteric regulator fructose-2,6-bisphosphate (Fig. 5b). Thus, secondary biochemical data confirm the inhibition mode that is suggested by the crystallographic data.

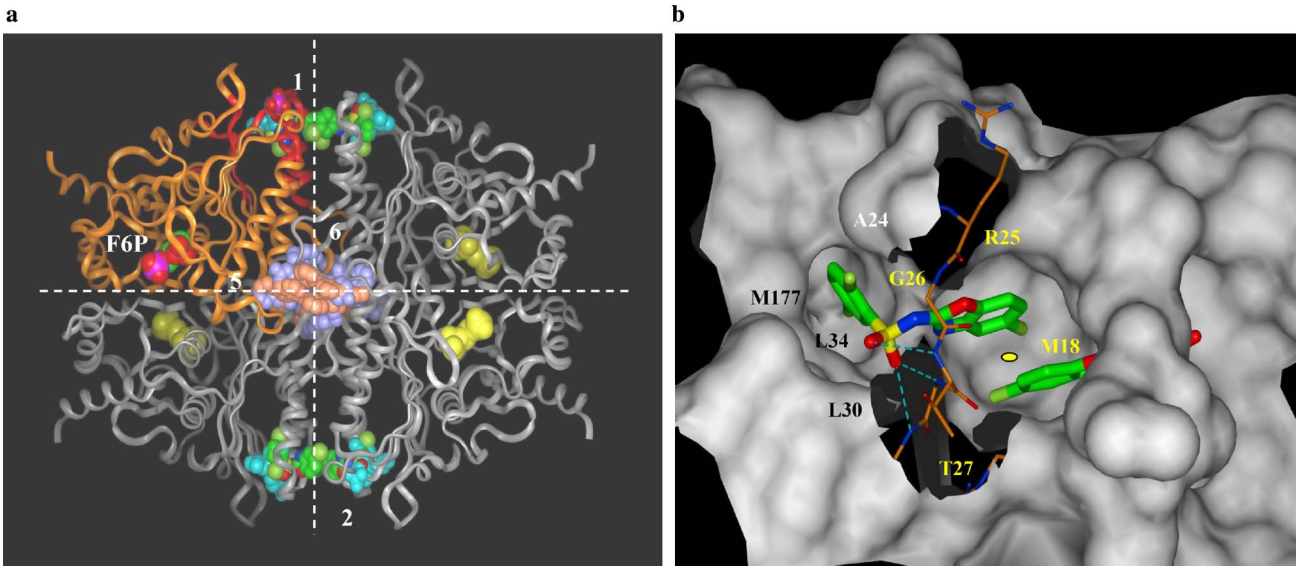

Figure 4. Crystallographic binding mode of various FBPase-1 inhibitors. (a) Binding modes of different FBPase-1 ligands, including fructose-6-phosphate (F6P). Symmetry axes are indicated with dashed lines. Compounds **5** (lt brown) and **6** (lt purple) bind with a stoichiometry of 2 per tetramer; all others bind at a stoichiometry of 4 per tetramer. Compounds **1** (atoms color coded) and **2** (cyan) overlap the AMP allosteric binding pocket. (b) Details of the interaction of **1** with the enzyme. In particular, **1** forms a dense network of H-bonds with the 'guardian bridge' that separates the AMP phosphate binding pocket from the subunit interface region. Highlighted residues serve to orient the viewer in the pocket and are not necessarily contact residues (see text for details). The yellow oval marks a symmetry axis; note the overlap of the benzoxazole rings of two molecules of compound **1** across this axis.

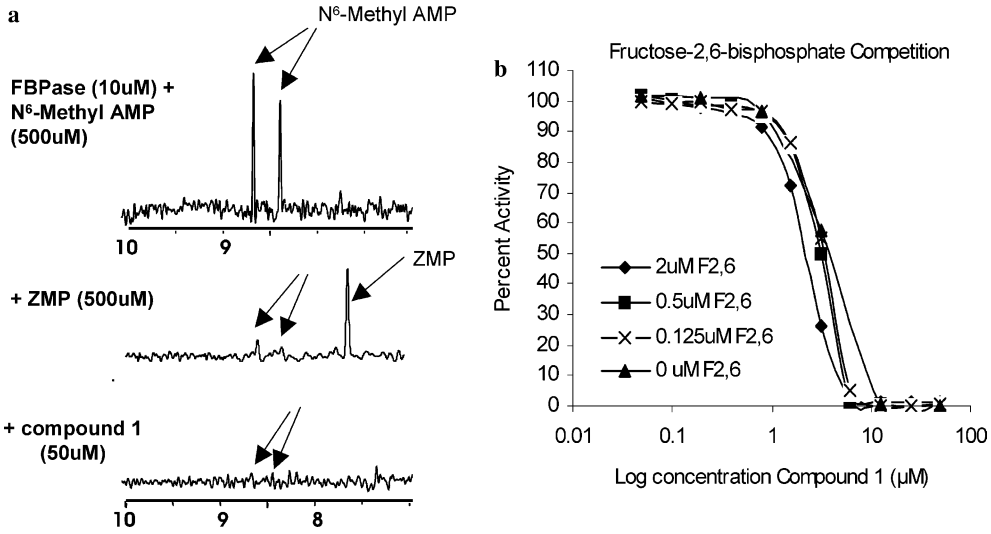

Figure 5. Interaction of **1** with other allosteric regulators of FBPase-1. (a) Addition of **1** suppresses energy transfer between the protein and N^6-methyl-AMP as measured by std-NMR, indicating that **1** competes for the AMP allosteric site. (b) Addition of fructose-2,6-bisphosphate fails to shift the inhibition curve of **1**, indicating that **1** does not compete for the F-2,6-bis-P binding site.

In conclusion, we have identified a novel class of inhibitors of FBPase-1, containing a benzoxazole-2-benzenesulfonamide as the key pharmacophore. Biochemical and structural studies indicate that prototype compound **1** has a novel binding mode which incorporates features that have been noted previously in several distinct inhibitor series. Like the heteroaryl phosphonates and indole diacids, the arylsulfonamide portion of **1** interacts with the AMP allosteric regulatory site; at the same time, the benzoxazole moiety protrudes into the interface between subunits of the FBPase homotetramer. To accommodate these distinct interactions, **1** must navigate a channel determined by the loop comprising residues Arg25 through Leu30. It accomplishes this by forming a unique web of H-bonding interactions between its hetero-dense sulfonamide core and the backbone amides along this channel. In subsequent articles, we will describe our studies to optimize the potency and ADME properties of this intriguing lead.

Acknowledgment

The authors thank Dr. Charles Hutchins for help generating the computer images provided herein.

References and notes

1. (a) McCormack, J. G.; Westergaard, N.; Kristiansen, M.; Brand, C. L.; Lau, J. *Curr. Pharm. Des.* **2001**, *7*, 1451; (b) Magnusson, I.; Rothman, D.; Katz, L.; Shulman, R.; Shulman, G. *J. Clin. Invest.* **1992**, *90*, 1323; (c) DeFronzo, R. A. *Diabetes Rev.* **1997**, *5*, 177; (d) Consoli, A.; Nurjhan, N.; Capani, F.; Gerich, J. *Diabetes* **1989**, *38*, 550.
2. (a) Hers, H. G.; Hue, L. *Annu. Rev. Biochem.* **1983**, *52*, 617; (b) Tejwani, G. A. *Adv. Enzyme* **1983**, *54*, 121.
3. (a) Rothman, D. L.; Magnusson, I.; Katz, L. D.; Shulman, R. G.; Shulman, G. I. *Science* **1991**, *254*, 573; (b) Andrikopoulos, S.; Rosella, G.; Kaczmarczyk, S. J.; Zajac, J. D.; Proietto, J. *Metabolism* **1996**, *45*, 622; (c) Wimhurst, J. M.; Manchester, K. L. *Biochem. J.* **1997**, *120*, 95.
4. (a) Gidh-Jain, M.; Zhang, Y.; van Poelje, P. D.; Liang, J.; Huang, S.; Kim, J.; Elliott, J. T.; Erion, M. D.; Pilkis, S. J.; El-Maghrabi, M. R.; Lipscomb, W. N. *J. Biol. Chem.* **1994**, *269*, 27732; (b) Choe, J.-Y.; Nelson, S. W.; Arienti, K. L.; Axe, F. U.; Collins, T. L.; Jones, T. K.; Kimmich, R. D. A.; Newman, M. J.; Norvell, K.; Ripka, W. C.; Romano, S. J.; Short, K. M.; Slee, D. H.; Fromm, H. J.; Honzatko, R. B. *J. Biol. Chem.* **2003**, *278*, 51176.
5. Erion, M. D.; van Poelje, P. D.; Dang, Q.; Kasibhatla, S. R.; Potter, S. C.; Reddy, M. R.; Reddy, K. J.; Jiang, T.; Lipscomb, W. N. *Proc. Natl. Acad. Sci. U.S.A.* **2005**, *102*, 7970.
6. Metabasis press release, September 26, 2003.
7. (a) Wright, S. W.; Carlo, A. A.; Danley, D. E.; Hageman, D. L.; Karam, G. A.; Mansour, M. N.; McClure, L. D.; Pandit, J.; Schulte, G. K.; Treadway, J. L.; Wang, I.-K.; Bauer, P. H. *Bioorg. Med. Chem. Lett.* **2003**, *13*, 2055; (b) Wright, S. W.; Carlo, A. A.; Carty, M. D.; Danley, D. E.; Hageman, D. L.; Karam, G. A.; Levy, C. B.; Mansour, M. N.; Mathiowetz, A. M.; McClure, L. D.; Nestor, N. B.; McPherson, R. K.; Pandit, J.; Pustilnik, L. R.; Schulte, G. K.; Soeller, W. C.; Treadway, J. L.; Wang, I.-K.; Bauer, P. H. *J. Med. Chem.* **2002**, *45*, 3865; (c) Wright, S. W.; Hageman, D. L.; McClure, L. D.; Carlo, A. A.; Treadway, J. L.; Mathiowetz, A. M.; Withka, J. M.; Bauer, P. H. *Bioorg. Med. Chem. Lett.* **2001**, *11*, 17.
8. Mjalli, A. M. M.; Mason, J. C.; Arienti, K. L.; Short, K. M.; Kimmich, R. D. A.; Jones, T. K. WO 99/47549 A1, 1999; *Chem. Abstr*. **1999**, *131*, 243287.
9. Conditions for malachite green assay: 2 mM $MgCl_2$, 150 mM NaCl, 0.1 mg/ml BSA, and 3 mM DTT in 50 mM Tris buffer; 400 ng/mL FBPase-1, 50 μM substrate. See Ref. 15 for further details.
10. Conditions for coupled assay: 2 mM $MgCl_2$, 150 mM KCl, 0.1 mg/ml BSA, and 0.1 mM EDTA in 50 mM HEPES buffer; 25 ng/mL FBPase-1, 1 U/mL PGI, 0.5 U/mL G6PDH, 5 μM substrate, and 200 μM NADP; continuous time-resolved format. See Ref. 16 for further details.
11. Crystallographic details: crystals of human FBPase-1 were grown under oil in the presence of ZMP ($K_i \sim 20$ μM) under conditions similar to the ones described by Ref.12. The seed compound (ZMP) was displaced by soaking the crystals in reservoir solution containing 10% glycerol with

1 mM compound **1**. The crystals were orthorhombic ($P2_12_12_1$) with cell constants $a = 84$, $b = 110$, $c = 190$ Å and diffracted to approximately 2.9 Å, using synchrotron radiation (Advanced Photon Source, APS, IMCA-CAT, 17-ID). The crystals contain one tetramer of FBPase and four molecules of **1** in the asymmetric unit. The structure was solved by molecular replacement and refined using standard methods. Crystallographic coordinates have been deposited at the Protein Data Bank with accession code 2fhy.

12. Zhu, D.-W.; Xu, G.-J.; Rehse, P. H.; Shi, R.; Zhao, F.-K.; Lin, S.-X. *Acta Cryst. D* **2001**, *57*, 847.
13. Mayer, M.; Meyer, B. *Angew. Chem. Int. Ed.* **1999**, *38*, 1784.
14. Vincent, M. F.; Erion, M. D.; Grube, H. E.; Van den Berghe, G. *Diabetologia* **1996**, *39*, 1148.
15. Baykov, A. A.; Evtushenko, O. A.; Avaeva, S. M. *Anal. Biochem.* **1988**, *171*, 266.
16. El-Maghrabi, M. R.; Gidh-Jain, M.; Austin, L. R.; Pilkis, S. J. *J. Biol. Chem.* **1993**, *268*, 9466.